PHILOSOPHICAL TRANSACTIONS OF THE ROYAL SOCIETY A MATHEMATICAL, PHYSICAL & ENGINEERING SCIENCES

Sea-going hardware for the cloud albedo method of reversing global warming

Stephen Salter, Graham Sortino and John Latham

Phil. Trans. R. Soc. A 2008 **366**, 3989-4006
doi: 10.1098/rsta.2008.0136

PHILOSOPHICAL TRANSACTIONS OF THE ROYAL SOCIETY A

Phil. Trans. R. Soc. A (2008) **366**, 3989–4006
doi:10.1098/rsta.2008.0136
Published online 29 August 2008

Sea-going hardware for the cloud albedo method of reversing global warming

By Stephen Salter[1,*], Graham Sortino[2] and John Latham[3]

[1]*Institute for Energy Systems, School of Engineering, University of Edinburgh, Edinburgh EH9 3JL, UK*
[2]*School of Informatics, University of Edinburgh, Edinburgh EH8 9AB, UK*
[3]*National Center for Atmospheric Research, Boulder, CO 80307-3000, USA*

Following the review by Latham *et al.* (Latham *et al.* 2008 *Phil. Trans. R. Soc. A* **366**) of a strategy to reduce insolation by exploiting the Twomey effect, the present paper describes in outline the rationale and underlying engineering hardware that may bring the strategy from concept to operation. Wind-driven spray vessels will sail back and forth perpendicular to the local prevailing wind and release micron-sized drops of seawater into the turbulent boundary layer beneath marine stratocumulus clouds. The combination of wind and vessel movements will treat a large area of sky. When residues left after drop evaporation reach cloud level they will provide many new cloud condensation nuclei giving more but smaller drops and so will increase the cloud albedo to reflect solar energy back out to space. If the possible power increase of 3.7 W m^{-2} from double pre-industrial CO_2 is divided by the 24-hour solar input of 340 W m^{-2}, a global albedo increase of only 1.1 per cent will produce a sufficient offset. The method is *not* intended to make new clouds. It will just make existing clouds whiter. This paper describes the design of 300 tonne ships powered by Flettner rotors rather than conventional sails. The vessels will drag turbines resembling oversized propellers through the water to provide the means for generating electrical energy. Some will be used for rotor spin, but most will be used to create spray by pumping 30 kg s^{-1} of carefully filtered water through banks of filters and then to micro-nozzles with piezoelectric excitation to vary drop diameter. The rotors offer a convenient housing for spray nozzles with fan assistance to help initial dispersion. The ratio of solar energy reflected by a drop at the top of a cloud to the energy needed to make the surface area of the nucleus on which it has grown is many orders of magnitude and so the spray quantities needed to achieve sufficient global cooling are technically feasible.

Keywords: global warming; Flettner rotor; Twomey effect; albedo control; cloud condensation nuclei; spray generation

1. Introduction

Other contributions to this volume by Caldeira & Wood (2008) and Rasch *et al.* (2008) examine the possibilities of injecting a sulphur aerosol into the upper layers of the stratosphere to increase albedo. Here, as proposed in the companion

* Author for correspondence (s.salter@ed.ac.uk).

One contribution of 12 to a Theme Issue 'Geoscale engineering to avert dangerous climate change'.

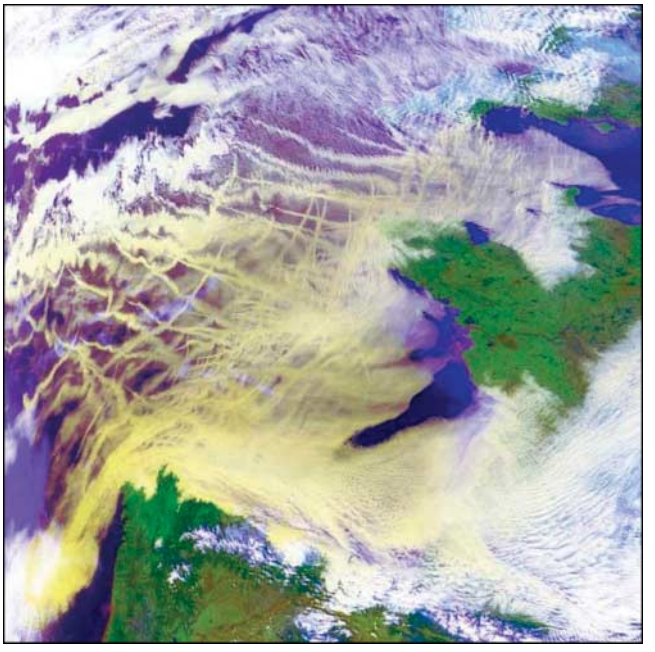

Figure 1. Demonstration of the Twomey effect. The photograph is a NASA satellite image of ship tracks over the Bay of Biscay. It was images such as this that triggered the Twomey work.

paper, Latham *et al.* (1990, 2002, 2008), and Bower *et al.* (2006), a different strategy is developed that exploits the Twomey effect, a striking, if inadvertent, demonstration of that which is provided in figure 1. Taken from a NASA satellite image, the long white streaks are caused by sulphates in the trails of exhausts from ship engines which provide extra condensation nuclei for new drops. Since, in the scheme we propose, the aim is to increase the solar reflectivity of such low-level maritime clouds and since a fine salt aerosol provides an admirable replacement for the sulphates whose effectiveness is evident in figure 1, it seemed appropriate for the sprays to be dispersed from sea-going vessels (rather than, say, low-flying aircraft) and for the source of the sprays to be drawn from the ocean itself. Thus, the present paper explores some of the design issues and concepts in using a fleet of wind-driven spray vessels to achieve the required albedo increase.

The first step in vessel design is to estimate the spray volumes needed. Cloud albedo $\boldsymbol{A}$ depends on cloud depth $\boldsymbol{Z}$ in metres, liquid water content $\boldsymbol{L}$, usually expressed in ml m^{-3}, and the concentration of cloud drops $\boldsymbol{n}$, usually expressed as the number per ml of air. For engineering purposes the equations in Twomey's classic paper (1977), usefully discussed by Schwartz & Slingo (1996), can be condensed by the use of a variable $\boldsymbol{K}(\boldsymbol{Z}, \boldsymbol{L}, \boldsymbol{n})$.

$$\text{If} \quad K(Z, L, n) \equiv 0.15\, ZL^{2/3} n^{1/3}, \tag{1.1}$$

then albedo

$$A(Z, L, n) = \frac{K(Z, L, n)}{K(Z, L, n) + 0.827}. \tag{1.2}$$

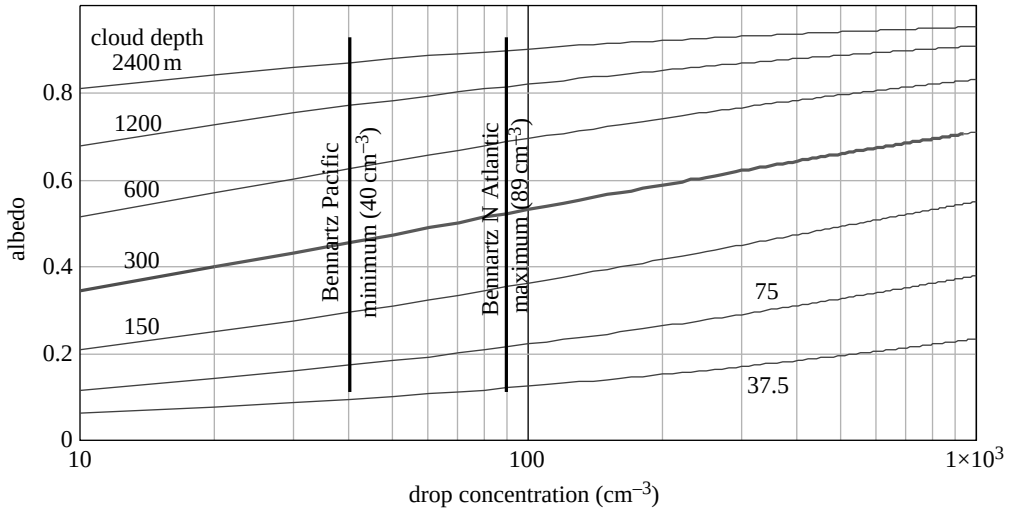

Figure 2. Cloud top reflectivity as a function of drop concentration for various cloud thicknesses and a liquid water content of 0.3 g m^{-3}. Adapted from Schwartz & Slingo (1996) with additions of the present range of concentrations for Pacific and Atlantic suggested by Bennartz (2007).

Following figure 2 of Schwartz & Slingo, this expression has been plotted in figure 2 of this paper against the concentration of cloud condensation nuclei for a typical liquid water content of 0.3 ml m^{-3} and for a wide range of cloud depths. The vertical black lines are the range of cloud drop concentrations for Pacific and North Atlantic given by Bennartz (2007). Changing the liquid water content by factors of 2 either way shifts the curves slightly downwards but because the slopes of the curves in the commonly occurring conditions are the same, this has little effect on the magnitude of the reflectivity change.

2. An atmospheric energy balance calculation

There is a vast amount of existing information on most of the parameters needed to calculate cooling as a function of spray rate, but it is distributed between many computers around the world and has been saved in different formats with different spatial resolutions and sampling rates, using different recovery software and different access protocols. Most of this information has now been collected, decoded, interpolated, unified and stored in a database as 6596 equal-area (7.72×10^{10} m^2) cells of a reduced Gaussian grid. This allows selective interrogation by an efficient parsing routine (Sortino 2006).

If there is to be double pre-industrial CO_2 with no temperature change, then solar reflection needs to increase by approximately 3.7 W m^{-2}, or 2000 Terawatts globally. This is about the electrical output of 1.8 million nuclear power stations of 1100 MW each. The question is how many spray vessels with how much spray equipment placed where at which season will be needed? Calculations can be done separately for each of the equal-area cells. The greatest uncertainties concern the estimates of the present number of cloud condensation nuclei at various times and places, and the drop lifetimes. This is because it is the *fractional change* in drop numbers in clouds that drives the change in albedo.

To demonstrate a spot test of equation (1.2) for reasonably typical conditions, let the cloud depth $\boldsymbol{Z}$ be 300 m, with a liquid water content $\boldsymbol{L}$ of 0.3 ml m^{-3} and use $\boldsymbol{n}=65$ cm^{-3} for the average mid-ocean drop concentration from the range of values suggested by Bennartz (2007) to calculate an albedo of $\boldsymbol{A}(\boldsymbol{Z}, \boldsymbol{L}, \boldsymbol{n})=0.495$.

The effect of injecting 30 kg s^{-1} of seawater as 0.8 μm drops but confining it to just one of the equal-area cells will be to increase the number of new nuclei per cell by 1.12×10^{17} s^{-1}. It will take some time (perhaps 2 hours) for turbulence to disperse the evaporated spray residues through the boundary layer, but the cleanliness of the mid-ocean air and the hydrophilic nature of the salty residue will make them very effective condensation nuclei. A large fraction of those that reach the high humidity at the cloud base will form newer but smaller drops with the same total liquid water content as before. It will take some further time before they wash out or coalesce with large drops. The lowest estimate for drop life is approximately 1 day, giving an increase of 9.67×10^{21} in each cell to bring the total to 1.47×10^{22}. The depth of the marine boundary layer is often between 500 and 1500 m. If we can take the depth of a cell of the reduced Gaussian grid to be 1000 m, the new concentration of cloud drops will be 191 cm^{-3}. This will make the new value of $\boldsymbol{A}(\boldsymbol{Z}, \boldsymbol{L}, \boldsymbol{n})=0.584$.

The mean 24-hour equinoctial solar input at the equator is 440 W m^{-2}, while at the latitude of Patagonia it is reduced to 240 W m^{-2}. If spray sources can migrate with the seasons, a typical value of 340 W m^{-2} seems reasonable, even conservative. The resulting change of albedo will increase reflected power by 30.26 W m^{-2} or 2.33 TW over the 7.72×10^{10} m^2 area of one cell.

We cannot be sure that spray sources will always be under the right kind of cloud. The most conservative cooling estimate would be based on the assumption of completely random, non-intelligent deployment of spray vessels. This would reduce the 2.33 TW cooling by the fraction of cover of suitable low-level stratocumulus. This is given by Charlson *et al.* (1987) as 0.18 and would reduce reflected power from a single source of 30 kg s^{-1}–420 GW. However, a lower concentration of nuclei over a wide area is more effective than a high one over a small area and the lifetime of nuclei under clear skies should be much longer than in cloud. It may turn out to be better to release spray in air masses that are cloudless but are predicted to become cloudy after some dispersal has taken place.

These crude engineering lumped calculations should be performed with the actual values at a representative sample of times for every cell that has not been excluded on grounds of being downwind of land with dirty air, upwind of drought-stricken regions or too close to busy shipping routes. The wind speed data for each cell should be checked to ensure that there is enough input power for, as will be developed shortly, wind energy provides the principal source for driving the vessels and creating the spray. With an efficient generator, the 30 kg s^{-1} flow rate will be reached at 8 m s^{-1} wind speed. If the nucleus lifetime was the longest estimate of 5 days (Houghton 2004), this would bring the concentration up to levels found over land and lead to much reduced effectiveness. Cells will be placed in rank order to see how many are needed to achieve any target cooling and either how many vessels should be put in each cell or how many cells should be treated by one vessel. Vessel movements can be planned by looking at the best-cell list for the next month.

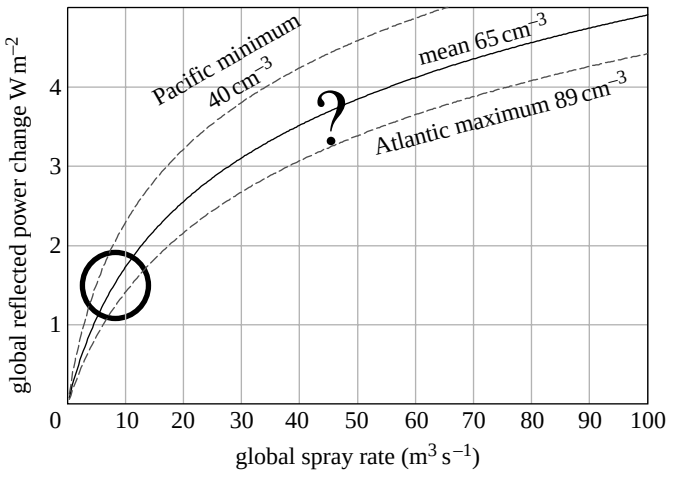

assumptions and sources

boundary layer depth	1000 m
cloud depth	300 m
	Schwartz and Slingo (1996)
liquid water	0.3 ml m^{-3}
	Schwartz and Slingo (1996)
drop life	59 h
	Smith *et al.* (1991)
low, not high, cloud fraction	0.18
	Charlson *et al.* (1987)
initial albedo	0.495
24 h power in	340 W m^{-2}

Figure 3. Global cooling as a function of spray rate for the assumptions in the right-hand side table, non-intelligent spraying and the range of initial nuclei concentration suggested by Bennartz (2007). The circle shows warming since the start of the industrial revolution. It could be reversed by spraying approximately 10 m^3 s^{-1}. The question mark is a guess for the effect of twice pre-industrial CO_2. Assumptions obtained from Charlson *et al.* (1987), Schwartz & Slingo (1996) and Smith *et al.* (1991).

The equations used for figure 2, together with lumped assumptions about what is in reality a wide spread of values, allow the approximate prediction of global cooling as a function of spray rate from purely randomly placed spray sources as shown in figure 3. The circle shows the approximate increase in positive forcing since the start of the industrial revolution. As the spraying rate is increased, the gain in reflected power evidently shows diminishing returns. But if these lumped assumptions are correct, the spray rate to cancel the 3.7 W m^{-2} effect of a doubling of pre-industrial CO_2 is between 30 and 70 m^3 s^{-1}.

It is also useful to calculate the spray amount that would 'hold the fort' long enough for renewable energy technologies to be deployed by cancelling the annual increase in global warming, probably approximately 40 mW m^{-2}. The annual increase would be a spray rate of less than 150 kg s^{-1}, even with non-intelligent positioning.

Suitable sites for spraying need plenty of incoming sunshine to give something to reflect. They must have a high fraction of low-level marine stratocumulus cloud. They should have few high clouds because these will reduce incoming energy and send the reflected energy down again. There should be reliable but not extreme winds to give spray vessels sufficient thrust. There should be a low density of shipping and icebergs. It helps to have a low initial density of cloud condensation nuclei because it is the fractional change that counts. This suggests sea areas distant from dirty or dusty land upwind. Owing to a possible anxiety over the effect of extra cloud condensation nuclei on rainfall, areas upwind of land with a drought problem should be avoided.

In figure 4 maps are for four seasons showing suitability of different sea areas based on the combination of one possible set of the selection criteria. Clearly, seasonal migration of the spray vessels is desirable and the southern oceans are particularly suitable for treatment in the southern summer. The very best all-year

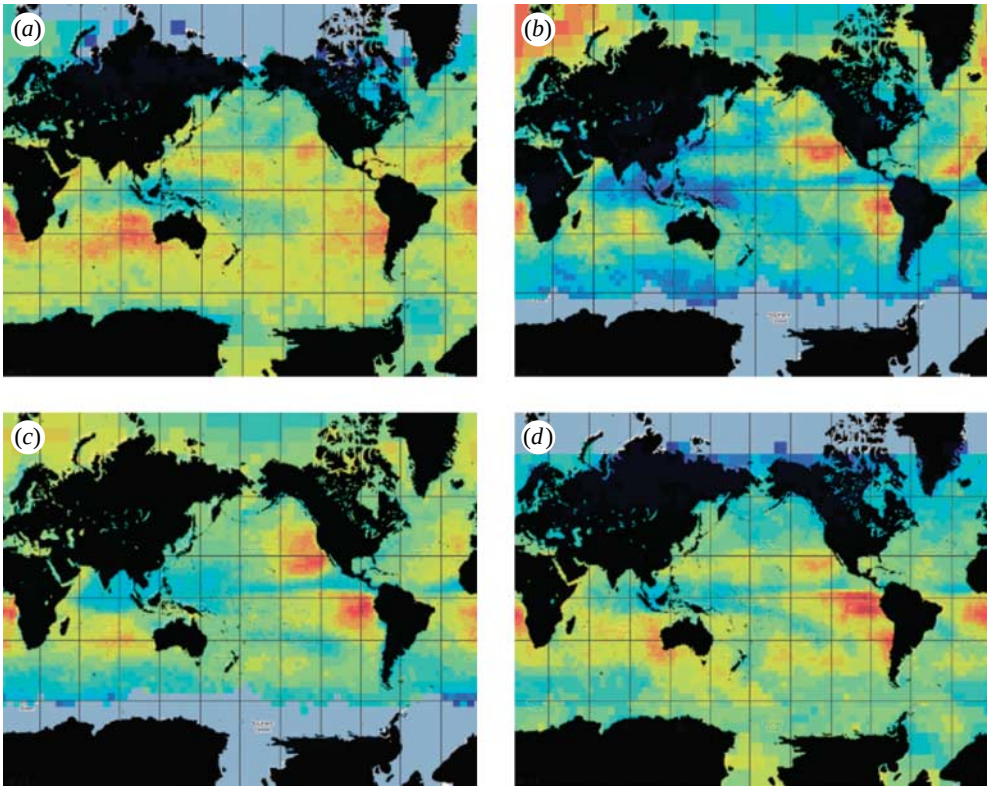

Figure 4. Results of a parameter combination based on a set of selection criteria of sunshine, initial CCN concentration, cloud cover and wind speed for four quarters of 2001 from Sortino (2006). Red is best but yellow is fine. Seasonal migration is indicated. (*a*) January–March, (*b*) April–June, (*c*) July–September and (*d*) October–December.

sites are off the coasts of California, Peru and Namibia. Regions in which marine currents are flowing towards the Arctic are of special interest partly because cooling this water might contribute to preserving Arctic ice cover, which is itself a powerful reflector of solar energy, and partly because a reduction in the release rate of methane from the melting of Siberian permafrost might be achieved.

3. Energy and propulsion

Energy is needed to make the spray. The proposed scheme will draw all the energy from the wind. Numbers of remotely controlled spray vessels will sail back and forth, perpendicular to the local prevailing wind. The motion through the water will drive underwater 'propellers' acting in reverse as turbines to generate electrical energy needed for spray production. Each unmanned spray vessel will have a global positioning system, a list of required positions and satellite communications to allow the list to be modified from time to time, allowing them to follow suitable cloud fields, migrate with the seasons and return to port for maintenance.

The problems of remotely operating and maintaining ropes, sails and reefing gear will be avoided, if the vessels use Flettner rotors instead of sails. These are vertical spinning cylinders that use the Magnus effect to produce forces

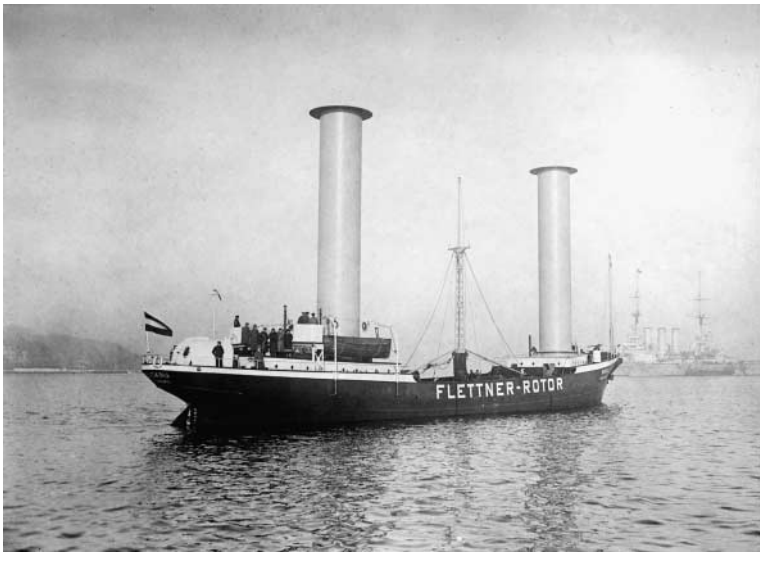

Figure 5. Anton Flettner's first rotor ship, the Baden-Baden, crossed the Atlantic in 1926.

perpendicular to the wind direction. Anton Flettner built two sea-going ships. The first, named Buckau, then renamed Baden-Baden (figure 5), crossed the Atlantic in 1926 (Seufert & Seufert 1983).

The rotors allow a sailing vessel to turn about its own axis, apply 'brakes' and go directly into reverse. They even allow self-reefing at a chosen wind speed. Flettner's rotor system weighed only one-quarter of the conventional sailing rig which it replaced. The rotor ships could sail 20° closer to the wind than unconverted sister ships. The heeling moment on the rotor flattened out in high wind speeds and was less than the previous bare rigging. With a wind on her quarter, the ship would heel *into* the wind. The only disadvantage of these vessels is that they have to tack to move downwind. Energy has to be provided for electric motors to spin the rotors, but this was typically 5–10 per cent of the engine power for a conventional ship of the same thrust. (After the Atlantic crossing, Flettner obtained orders for six more. He built one, Barbara, but had the rest cancelled as a result of the 1929 depression.) Flettner used drums of steel and, later, aluminium. Today much lighter ones could be built with Kevlar or carbon-reinforced epoxy materials. His main problem seems to have been to find bearings capable of taking the large aerodynamic forces at quite high velocities despite the geometric distortions of heavily loaded structures. The development by SKF of geometrically tolerant rolling bearings will have removed many of the difficulties. A major wind-turbine manufacturer, Enercon, is said to be launching a Flettner rotor ship in 2008. She will have four rotors, 4 m in diameter and 27 m tall.

4. Rotor lift and drag

The lift forces of a spinning cylinder are very much higher than those of a textile sail or an aircraft wing having the same projected area. Potential theory predicts that the lift per unit length of rotor should be 2π times the product of the

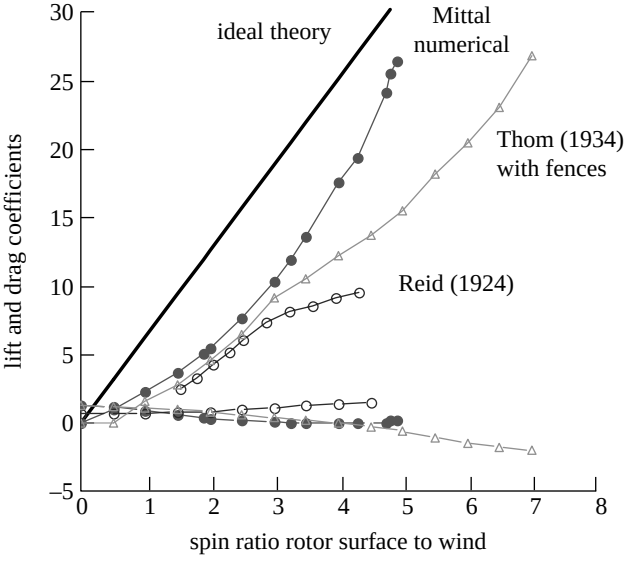

Figure 6. A collection of measured and calculated lift and drag coefficients for spinning cylinders.

surface speed of the rotor and far-field wind speed. This means that, for a constant rotor speed, it will rise with the *first* power of wind speed rather than with the square. If rotor surface speed and wind speed are kept in proportion, square law equations can be used (as in aircraft design) for comparison with wings and sails. The spin ratio (defined as local rotor speed over far-field wind speed in a frame moving with the vessel) acts such as the angle of incidence of the aerofoil section of an aircraft wing. The lift coefficient from ideal potential theory, as used with the square of velocity in aircraft design, is shown as the heavy line of figure 6. The open circles are from wind tunnel tests by Reid (1924) on a 115 mm diameter cylinder. He reported excessive vibration sufficient to stop the test at 3000 r.p.m. and a tunnel speed of 10 m s^{-1}, which would be a spin ratio of 1.79, but did not report results for spin ratios above 4.32.

It is well known that part of the drag on an aircraft wing is due to the permanent tip vortex generated by the positive pressure on the under surface driving air to the negative pressure on the upper surface. The effect can be minimized by high aspect-ratio wings, such as those of the albatross, and by tip fins. It was for this reason that Flettner added discs to the tops of his rotors (see figure 5). As a further design development, Thom (1934) experimented with multiple discs (or fences) and found that they produced very much higher lift coefficients and sometimes even negative drag coefficients. His data for disc diameters three times the rotor diameter placed at intervals of 0.75 of the rotor diameter are plotted as open triangles.

The negative drag coefficients imply that some forward drive power is being taken from the rotor drive. Also plotted in figure 6 with filled circles are coefficients from a numerical simulation carried out by Mittal & Kumar (2003) for an infinitely long cylinder. The falling drag values, even going negative, are of interest and provide qualitative support for Thom's observations. All predictions agree quite well up to spin ratios of approximately 3, but diverge for higher

values. A photograph of a sea-going yacht conversion by John Marples incorporating Flettner rotors with Thom fences is shown in figure 7. An artist's impression of the final spray vessel is shown in figure 8.

Wind tunnel balances from the pre-war years had none of the force-sensing transducers allowed by later electronics. It must have been difficult to make accurate small drag-force measurements on vortex shedding rotors that were being fed with mechanical power. But if Mittal and Thom are right, we can design some very exciting sailing ships.

Figure 9, also taken from Mittal and Kumar, shows lift coefficients against time after spin-up for a series of spin ratios from 0 to 5. There is an interesting build up of vibrations for spin ratios up to 2 and also between 4 and 4.8 which are reminiscent of vortex shedding and are in good agreement with Reid's reported vibrations. (As a cautionary note, however, the Reynolds number in Mittal and Kumar's simulations is only 200, so there must be some doubt as to whether the same features will be present in a full-scale craft where the Reynolds numbers will be at least four orders of magnitude greater.)

In a subsequent paper, Mittal (2004) shows span-wise axial oscillations in air velocity at various times after spin-up. The pitch of the oscillations is close to that of the fences suggested by Thom and it may be that the superior performance of fenced rotors is caused by the suppression of this instability. Thom measured the torque needed to spin his cylinders, but then made a mistake in scaling up the torque coefficient to the much higher Reynolds numbers needed for practical applications. This was spotted by Norwood (1991), who confirmed his own torque calculations with a model test.

The patterns of the air flow associated with the vibrations of Mittal's numerical predictions show clear vortex shedding as in the flow over a stalled aircraft wing. The vortex axes are parallel to the spin axis. Some aircraft designers put small vortex generators on the upper wing surfaces to induce pairs of vortices with axes parallel to the line of flight. These stabilize the air flow against separation. A single disc will centrifuge air outwards and lose all its kinetic energy. But perhaps closely packed discs with root fillets, as in figure 8, may also induce pairs of vortices returning some of the kinetic energy of spin to the rotor core. The resistance to buckling of the double curvature of the fillets on the discs will make them much stronger.

5. Spray generation

Provided that salt residues are of sufficient size to achieve nucleation, it is the *number* of drops rather than the mass of spray which matters. The aim is a monodisperse spray with a diameter of 0.8 μm but with the option for some controlled diameter variation. Spinning discs, ultrasonic excitation of Faraday waves and colliding jets of high-pressure water/air solutions have all been studied. The final choice uses silicon micro-fabrication technology. A hexagonal array of 1483 submicron holes will be etched through an 8 μm layer of silicon to meet a 50 μm hole through the thickness of a 0.5 mm wafer. This will be repeated 1345 times within the area of a 3.2 mm hole in a Yokota YST130N stainless steel disc. This hole will be one of 499 spread across a 100 mm wafer to give nearly 10^9 micro-nozzles in each of the 18 wafers of a spray vessel. Ultrasonic excitation

Figure 7. John Marples' Cloudia (a rebuilt Searunner 34), with Thom fences on test at Fort Pierce, FL, February 2008. With a rotor drive power of 600 watts, she could sail faster than the beam wind, stop, go into reverse and yaw 180° in either direction about her own axis. Funding for work on Cloudia was provided by the Discovery Channel and organized by Impossible Pictures. © Discovery Channel.

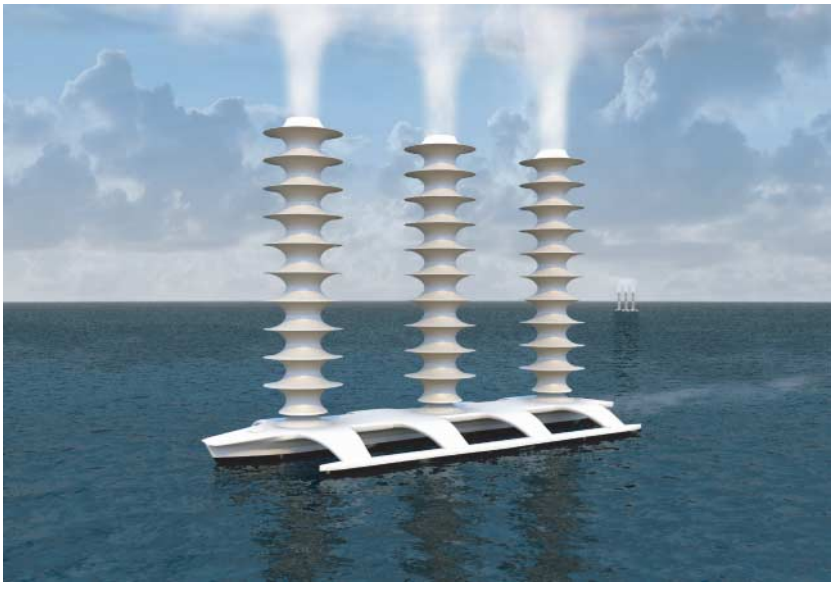

Figure 8. A conceptual Flettner spray vessel with Thom fences. The wind would be blowing from the reader's right-hand side, the rotor spin would be clockwise seen from above and rotor thrust to the left. Vessels can also report sea and air temperatures, humidity, solar input, the direction and velocities of winds and currents, atmospheric pressure, visibility, cloud cover, plankton count, aerosol count, salinity, radio reception and could even rescue yachtsmen in distress (copyright © J. MacNeill 2006).

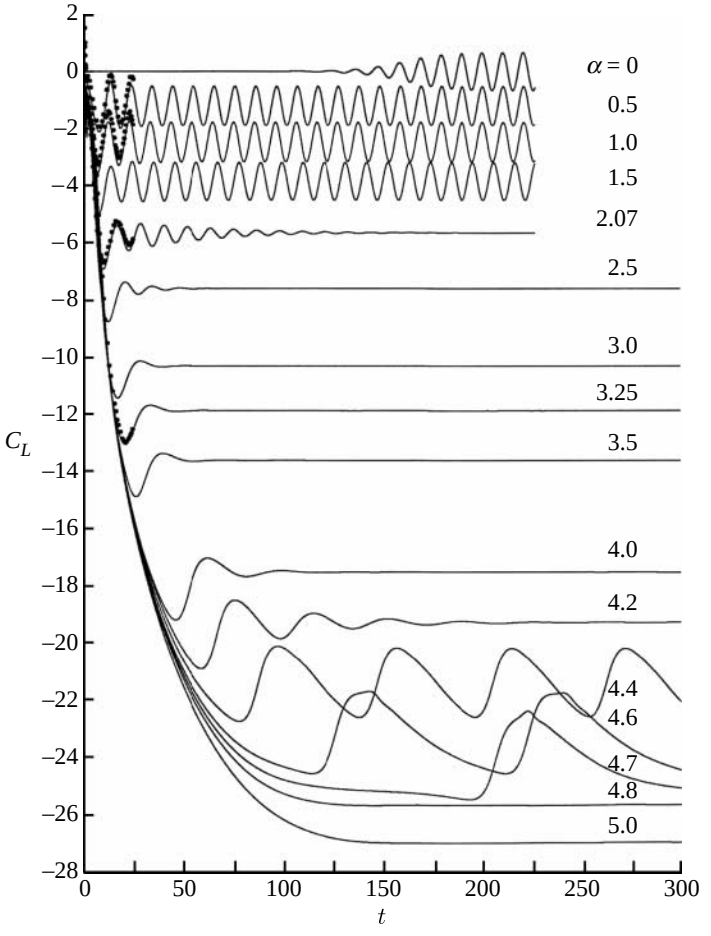

Figure 9. Numerical lift coefficients versus time (Mittal & Kumar 2003). Courtesy of *Journal of Fluid Mechanics*.

can be used to reduce drop size from the value predicted by Rayleigh (1878). The silicon will be protected by an oxide layer sealed with vapour-deposited Parylene. Energy losses are dominated by the viscosity through the 8 μm layer. The nozzle banks must be drenched in desalinated water when the system is idle.

A weakness of the micro-nozzle approach is that particles much smaller than a nozzle can form an arch to clog it. Fortunately, the need to remove viruses from ground water for drinking purposes has produced a good selection of ultrafiltration products that can filter to a better level than is needed. Suppliers guarantee a life of 5 years provided that back-flushing can be done at the right intervals. Each rotor has a Grundfoss down-hole pump that feeds 17 $m^3\,s^{-1}$ to a bank of eight filters with blister valves to allow any filter to be back-flushed. Norit X-flow filters have an excellent record for pre-filtration in reverse osmosis desalination plant (van Hoof *et al.* 1999). A trash-grid made from titanium mesh will prevent jelly fish and plastic bags from jamming the pump. If it is fed with a current of 90 amps, it can also produce 2 ppm electrolytic chlorine to prevent biological growths.

Electrical energy for spray and rotor drive will be generated by a pair of 2.4 m diameter axial-flow turbines on either side of the hull as shown in figure 10. These are very much larger than any propellers needed for a vessel of this size but can act as propellers for 10 hours in windless conditions using energy from a bank of Toshiba SCiB batteries. The vessels will also carry a liquid-cooled version of the Zoche ZO 01A radial diesel aero engine to give trans-ocean range in emergency. The turbine rotation speed will be limited by cavitation to approximately 80 r.p.m. This is fast enough for the use of polyphase permanent-magnet rim generators built into the turbine ducts. Tiles of neodymium-boron magnets will be moved past wet printed-circuit pancake stator windings sealed in glass-flake epoxy Parylene. The axial thrust on the rotor is taken by a pair of 45° SKF spherical roller thrust bearings aft of the rotor and an SKF CARB bearing at the forward end.

6. Rotor design

Rotor dimensions of 20 m height and 2.4 m core diameter are chosen to produce a thrust sufficient for full turbine power in a wind speed of 8 m s^{-1} and look very small compared with conventional sails. The difficult region is at the root of the internal mast where the design must resolve the many conflicts between

— the transfer of large thrust forces and moments from the mast to the hull;
— the possible need to deal with wave impact;
— the need to send water to the spray-release system;
— the transmission of drive torque to the rotors at variable speeds in either direction;
— the pumping of a large volume of air through the rotors for spray dispersion; and
— the need to allow extension and deflection of the rotor and mast by some form of universal joint with radial and torsional stiffness but with the freedom for the rotor to distort in heave, roll and pitch.

The main thrust and the weight of the motor are taken by a pair of 45° spherical roller bearings placed slightly below half the height of the rotor. Forces due to uneven aerodynamic loads and roll acceleration are taken through a tri-link mechanism at the bottom of the rotor to a pair of angular-contact ball bearings matched for low swash play. The tri-link allows the rotor to stretch and bend without loading the bearings. It turns out that the design is rigidity limited to stay within the acceptable angular movement of the spherical bearings rather than being strength limited. The drive motor, shown in figure 11, has a 1 m hole and is built around outside of the mast. It is made with moving magnets and a pancake stator, very similar to that of the turbine.

Spray will be released just above the upper bearing into an upward airstream of 12 m s^{-1} produced by fan blades just below the upper bearing. The fan blade angle has to change when rotor direction changes to allow the vessel to go about. The air passage at the bottom of the rotor is narrowed by a factor of 4, so that the Bernoulli pressure drop can provide suction for the rotor surface to prevent flow separation as shown by Prandtl in 1904 (see Braslow *et al.* 1951; Schlichting 1979, ch. 14). Motor drive torque is based on fan requirements and reverse

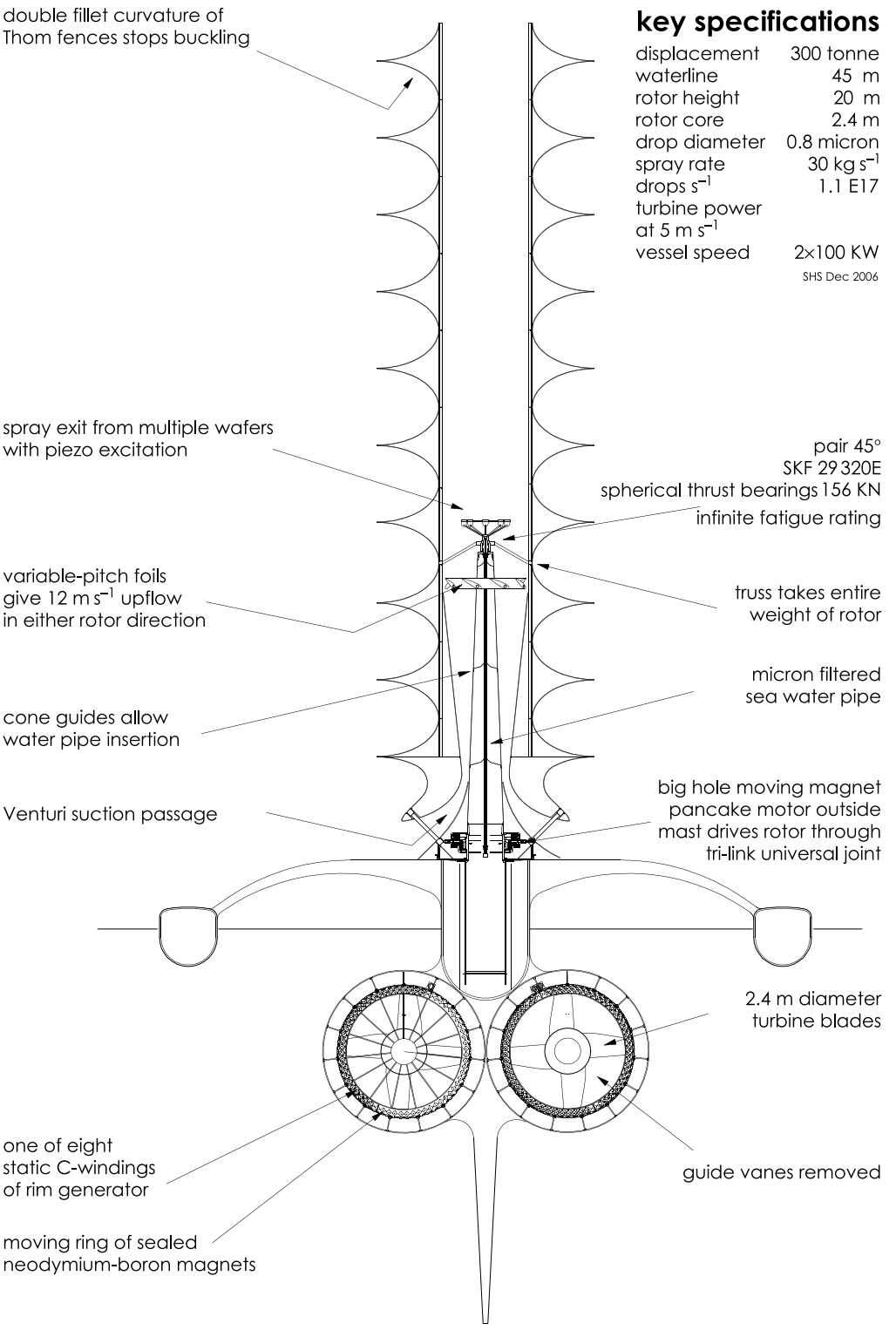

Figure 10. A cross-sectional view through rotor and turbines.

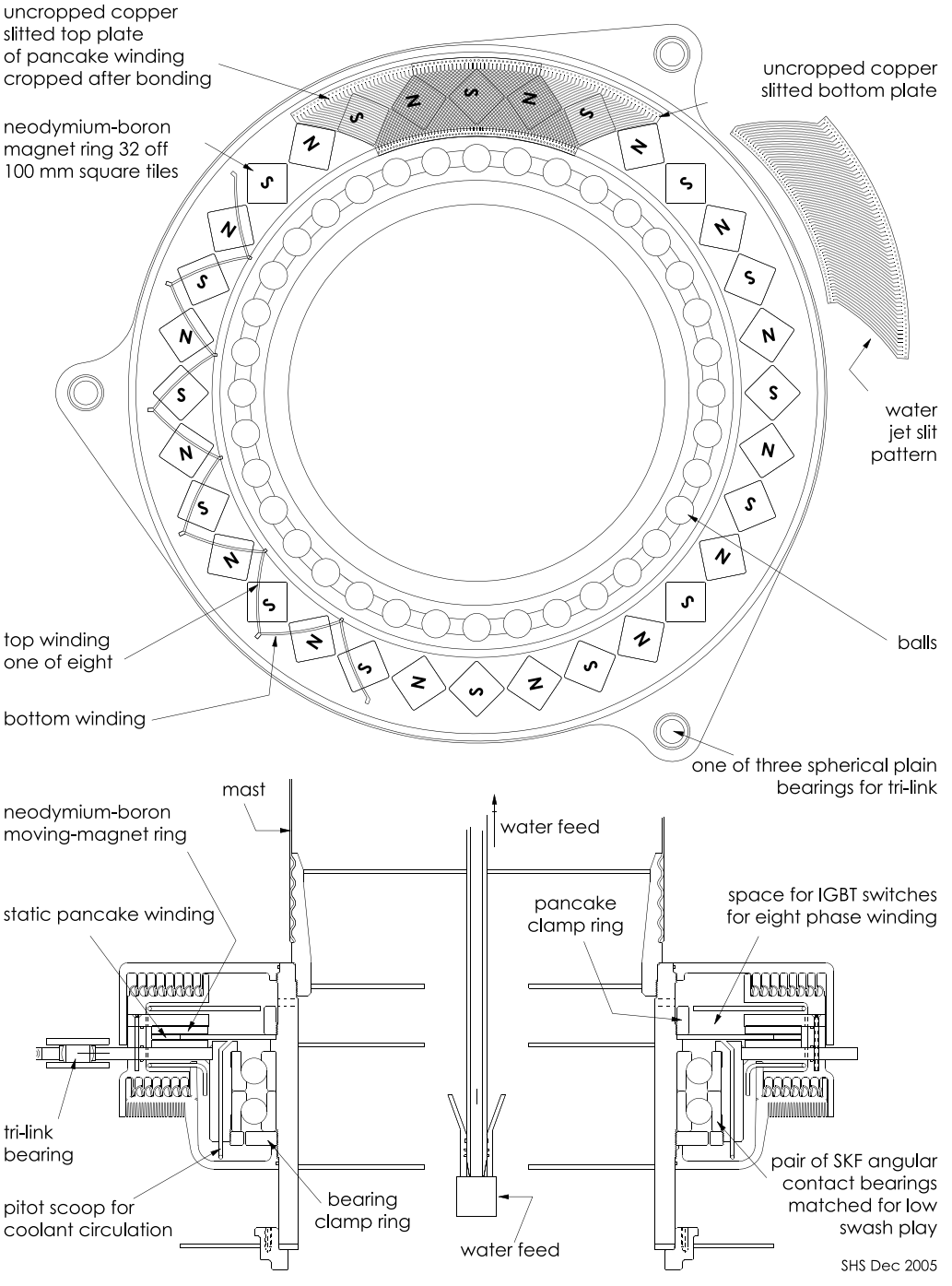

Figure 11. A motor with a hole large enough to fit outside the mast solves the conflicts between rotor loads, torque drive and water pipes.

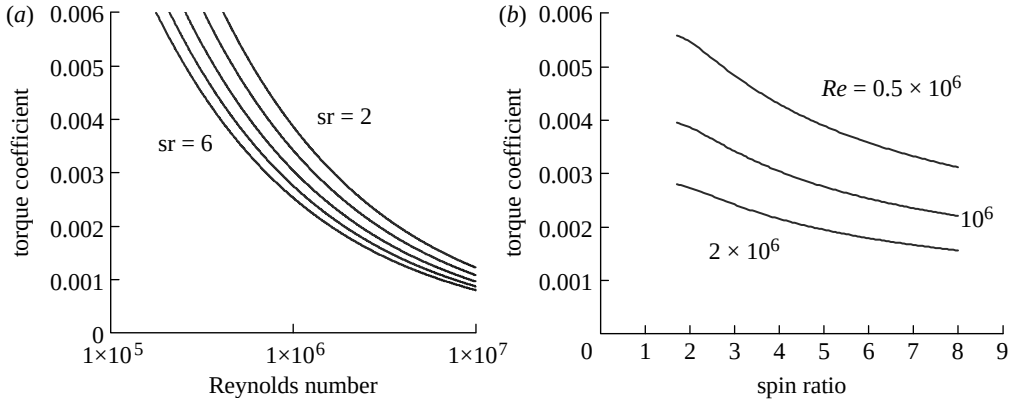

Figure 12. (*a*) Glauert's torque coefficients against Reynolds number for spin ratios 2–6 and (*b*) against spin ratio for Reynolds numbers 0.5, 1 and 2 million. Flettner used a safety factor of 2 and so shall we. But if the suction idea works, we can hope for even lower drive torque requirements.

engineering the quoted drive power values from Flettner ships which indicate torsional drag coefficients of approximately 0.006. This is above that predicted by Glauert (1957) and Padrino & Joseph (2006), as shown in figure 12.

7. Project costs

A development programme has been planned to reduce technical uncertainties. These mainly involve the design of an efficient spray generator, a study of drop life and dispersion, a study of the present distribution of cloud condensation nuclei, a limited-area field experiment and rigorous meteorological modelling, especially of any adverse effects. Very few uncertainties will remain after the expenditure of the first £2 million over 2 years. It will need perhaps £25 million and a further 3 years to complete research and development of the reliable hardware for spray vessels including the first fully instrumented, full-scale, crewed and sea-going prototype. Once there is experience of its operation, it will cost approximately £30 million for tooling, which will allow a large number of spray vessels to be built rapidly in the event of a global emergency.

The vessels are expected to have a displacement of 300 tonnes and a plant rating of 150 kW. Much industrial equipment costs approximately £1000 kW^{-1}. Medium-sized ships cost approximately £2000 tonne^{-1} dead weight. Smaller ones may be more expensive. It seems likely that production spray vessels will cost between £1 and £2 million each.

Most small- and medium-sized yachts are now built with glass-reinforced plastic. The expected displacement of the present vessels may be above the size for which this material is suitable and so the first prototype is being designed for steel construction, which is convenient for subsequent modifications involving extra holes and welded attachments. Alternatively, an attractive material for mass production would be ferrocement owing to its excellent long-term resistance to seawater. There is also a growing number of interesting plastic-reinforced cement materials which should be considered.

Filter manufacturers will guarantee a 5-year life and expect that most will last for 10 years. Enough is known about bearing loads to achieve long life and the main unavoidable maintenance cost will be anti-fouling treatments. For ships moving continuously in cold water, anti-fouling intervals will be longer than for ones frequently moored in warm harbours. These figures suggest that eventually the maintenance will be low in comparison with return on capital.

If world temperatures are to be kept steady with no carbon reduction, the working fleet would have to be increased by approximately 50 vessels a year plus extra ones to replace any lost. If the assumptions used for figure 3 are correct, the cancellation of $3.7\,\mathrm{W\,m^{-2}}$ associated with a doubling of pre-industrial CO_2 will need a spray rate of approximately $45\,\mathrm{m^3\,s^{-1}}$ and perhaps less with skilful vessel deployment. If $0.03\,\mathrm{m^3\,s^{-1}}$ is the right design choice for one spray vessel, this could come from a working fleet of approximately 1500.

8. Conclusions

It is possible that a fleet of remotely controlled wind-driven spray vessels can exploit the Twomey effect to make useful reductions to the input of solar energy to the sea. It can also provide valuable meteorological and oceanographic data.

The Flettner rotor, perhaps with Thom fences, is an attractive alternative to sails owing to its high-lift coefficients and high lift–drag ratios but mainly for easy control by computer and the convenience for housing spray plant producing an upward air flow.

Long-life ultrafiltration modules can deliver seawater with absolute filtration below 0.1 μm but with the salt still present. This will not clog 0.8 μm nozzles manufactured in silicon wafers using lithographic techniques from the micro-fabrication industry. So far, this seems to be the most energy-efficient spray system that can be devised. With stronger notch-tolerant materials for the nozzle grid, the energy requirement can approach the absolute minimum needed for creation of new surface area against the force of surface tension.

Predictions for global cooling power as a function of spray rate depend strongly on assumptions of initial concentration of condensation nuclei and the lifetime of spray but only weakly on cloud liquid–water content and depth. It is possible that 50 spray vessels costing approximately £1–2 million each could cancel the thermal effects of a 1-year increase in world CO_2.

The immediate effect of albedo control is local cooling of the sea surface. It could be targeted at vulnerable regions, such as coral reefs and diminishing polar ice. It may reduce the frequency and severity of hurricanes and extend the sea area suitable for phytoplankton growth. However, the oceans are an effective thermal store, and currents are an efficient transport mechanism, so initial effects will eventually spread world wide.

Sea temperatures have a strong influence on world climate. Initially, the deployment of spray vessels in an attempt to replicate favourable historic oceanic temperature patterns will delay the need for perfect understanding of all the many complicated interactions.

Spray releases with control of time, place, quantity and drop diameter will give atmospheric physicists a rare chance to try controlled experiments and so help in the understanding of atmospheric aerosols that have such powerful effects on climate.

While a major effort should be put into the study of all possible side effects of keeping sea temperatures at present values (or other values of our choosing), many of the side effects appear to be benign and less dangerous than those of large, unbridled temperature rises. Unsuitable places can be avoided and spraying can be stopped instantly with all effects removed in a few days.

Albedo control can do nothing for ocean acidity.

All geoengineers have been inspired by the pioneering work of James Lovelock. Key suggestions about spray generation are due to Lowell Wood and Tom Stevenson. NASA and the ISCCP have been extremely generous with information and patient in explaining how we can use it. Their continued work on understanding and protecting the home planet has earned respect and admiration from many countries round the world. Funding for work on Cloudia was provided by the Discovery Channel and organized by Impossible Pictures. The National Center for Atmospheric Research is sponsored by the National Science Foundation. Any opinions, findings and conclusions or recommendations expressed in this publication are those of the authors and do not necessarily reflect the views of the National Science Foundation.

References

Bennartz, R. 2007 Global assessment of marine boundary layer cloud droplet number concentration from satellite. *J. Geophys. Res.* **112**, D02201. (doi:10.1029/2006JD007547)

Bower, K., Choularton, T., Latham, J., Sahraei, J. & Salter, S. 2006 Computational assessment of a proposed technique for global warming mitigation via albedo-enhancement of marine stratocumulus clouds. *Atmos. Res.* **82**, 328–336. (doi:10.1016/j.atmosres.2005.11.013)

Braslow, A. L., Burrows, D. L., Tetervin, N. & Viscconti, F. 1951 Experimental and theoretical studies of area suction for the control of the laminar boundary layer. NACA Report 1025.

Caldeira, K. & Wood, L. 2008 Global and Arctic climate engineering: numerical model studies. *Phil. Trans. R. Soc. A* **366**, 4039–4056. (doi:10.1098/rsta.2008.0132)

Charlson, R. J., Lovelock, J. E., Andreae, M. O. & Warren, S. G. 1987 Oceanic phytoplankton, atmospheric sulphur and climate. *Nature* **326**, 655–661. (doi:10.1038/326655a0)

Glauert, M. B. 1957 The flow past a rapidly rotating cylinder. *Proc. R. Soc. A* **242**, 108–115. (doi:10.1098/rspa.1957.0157)

Houghton, J. 2004 *Global warming, the complete briefing.* Cambridge, UK: Cambridge University Press.

Latham, J. 1990 Control of global warming. *Nature* **347**, 339–340. (doi:10.1038/347339b0)

Latham, J. 2002 Amelioration of global warming by controlled enhancement of the albedo and longevity of low-level maritime clouds. *Atmos. Sci. Lett.* **3**, 52. (doi:10.1006/asle.2002.0048)

Latham, J., Rasch, P., Chen, C.-C. J., Kettles, L., Gadian, A., Gettelman, A., Morrison, H., Bower, K. & Choularton, T. 2008 Global temperature stabilization via controlled albedo enhancement of low-level maritime clouds. *Phil. Trans. R. Soc. A* **366**, 3969–3987. (doi:10.1098/rsta.2008.0137)

Mittal, S. 2004 Three dimensional instabilities in flow past a rotating cylinder. *ASME J. Appl. Mech.* **71**, 89–95.

Mittal, S. & Kumar, B. 2003 Flow past a rotating cylinder. *J. Fluid Mech.* **476**, 303–334. (doi:10.1017/S0022112002002938)

Norwood, J. 1991 Performance prediction for 21st century multihull sailing yachts. London, UK: Amateur Yacht Research Association. (http://www.ayrs.org/)

Padrino, J. C. & Joseph, D. D. 2006 Numerical study of the steady state uniform flow past a rotating cylinder. *J. Fluid Mech.* **557**, 191–223. (doi:10.1017/S0022112006009682)

Rasch, P. J., Tilmes, S., Turco, R. P., Robock, A., Oman, L., Chen, C.-C. J., Stenchikov, G. L. & Garcia, R. R. 2008 An overview of geoengineering of climate using stratospheric sulphate aerosols. *Phil. Trans. R. Soc. A* **366**, 4007–4037. (doi:10.1098/rsta.2008.0131)

Rayleigh, L. 1878 On the instability of jets. *Proc. Lond. Math. Soc.* **S1–10**, 4–13. (doi:10.1112/plms/s1-10.1.45)

Reid, E. G. 1924 Tests of rotating cylinders. Technical notes NACA-TN-209.

Schlichting, H. 1979 *Boundary layer theory*. New York, NY: McGraw-Hill.

Schwartz, S. E. & Slingo, A. 1996 Enhanced shortwave radiative forcing due to anthropogenic aerosols. (Intelligible even to engineers.) In *Clouds chemistry and climate* (eds P. Crutzen & V. Ramanathan), pp. 191–236. Heidelberg, Germany: Springer.

Seufert, W. & Seufert, S. 1983 Critics in a spin over Flettner's ship. *New Sci.* 656–659.

Smith, M. H., Park, P. M. & Consterdine, I. E. 1991 North Atlantic aerosol remote concentrations measured at a hebridean coastal site. *Atmos. Environ. A* **25**, 547–555. (doi:10.1016/0960-1686(91)90051-8)

Sortino, G. 2006 A data resource for cloud cover simulation. MSc thesis, School of Informatics, University of Edinburgh.

Thom, A. 1934 Effects of disks on the air forces on a rotating cylinder. Aeronautical Research Committee Reports and Memoranda 1623. (Available from Cranfield University NACA archive.)

Twomey, S. 1977 Influence of pollution on the short-wave albedo of clouds. *J. Atmos. Sci.* **34**, 1149–1152. (doi:10.1175/1520-0469(1977)034<1149:TIOPOT>2.0.CO;2)

Van Hoof, S. C. J. M., Hashim, A. & Kordes, A. J. 1999 The effect of ultrafiltration as pretreatment to reverse osmosis in wastewater reuse and seawater desalination applications. *Desalination* **124**, 231–242. (doi:10.1016/S0011-9164(99)00108-3)